Materials Today Bio 33 (2025) 102032

Contents lists available at ScienceDirect

Materials Today Bio

journal homepage: www.journals.elsevier.com/materials-today-bio

Modular design of biomimetic electrospun keratin composites for tunable gaseous sorption inspired by reptile eggshells

Yana Maudens [a], Gerben Debruyn [b], Eva Loccufier [a], Lode Daelemans [a], Erica Savino [c], Cinzia Tonetti [c], Claudia Vineis [c], Alessio Varesano [c], Matthew D. Shawkey [b], Liliana D'Alba [b,d,*], Karen De Clerck [a,**]

[a] Ghent University, Department of Materials Textiles and Chemical Engineering, Center for Textile Science and Engineering, Tech Lane Science Park 70A, Ghent, 9052, Belgium
[b] Ghent University, Department of Biology, Evolution and Optics of Nanostructures Group, Karel Lodewijk Ledeganckstraat 35, Ghent, 9000, Belgium
[c] National Research Council-Institute of Intelligent Industrial Technologies and Systems for Advanced Manufacturing (CNR-STIIMA), Corso Giuseppe Pella 16, Biella, 13900, Italy
[d] Naturalis Biodiversity Center, Darwinweg 2, CR, Leiden, 2333, Netherlands

ARTICLE INFO

Keywords:
Modular biomimetic composites
Protein nanofibers
Keratin electrospinning
Tunable vapor sorption
Reptile eggshells

ABSTRACT

Biomimicry, the replication of natural structures, is an emerging strategy in materials engineering for developing advanced functional materials. Reptile eggshells serve as compelling models for tunable bioinspired material design due to their diversity in forms and functions. This study presents a modular approach to designing keratin-based composites with customizable vapor sorption behavior. Inspired by reptile eggshells, four key biomimetic components were reconstructed: (1) electrospun keratin membranes resembling the fibrous shell membrane, (2) an egg protein matrix replicating the proteinaceous eggshell matrix, (3) calcium carbonate ($CaCO_3$) particles introducing mineralization, and (4) a paraffin coating representing the lipid-rich cuticle layer. The modular accuracy of these biomimetic models was validated by comparison with representative reptile eggshells through Scanning Electron Microscopy analysis and Fourier-Transform Infrared Spectroscopy. Dynamic Vapor Sorption (DVS) analysis confirmed that varying the $CaCO_3$ content allows precise control over the absorption profiles, ranging from low to high sorption values. Additionally, integrating the organic matrix and lipid coating enabled fine-tuning of the sorption properties. The resulting biomimetic composites exhibited sorption characteristics comparable to those of natural eggshells, including *Caiman crocodilus* (low absorption) and *Pantherophis guttatus* (high absorption), demonstrating the effectiveness of the modular design strategy. These findings establish a foundation for engineering advanced biocompatible materials with adaptable sorption behavior, offering potential applications in moisture-regulating wound dressings, tissue engineering scaffolds, sustainable packaging, and filtration systems.

1. Introduction

Biomimicry—the process of studying nature, deriving working principles, and applying them to replicate biological systems—is a fascinating strategy in materials science to develop advanced functional materials [1,2]. Reptile eggshells serve as compelling models for bio-inspired material design due to their diversity in form and function [3–7]. Unlike the relatively uniform structure of avian eggshells, reptile eggshells display a wide range of configurations driven by the wide range of breeding conditions and environmental pressures encountered across reptilian species [3,8,9]. A limited set of building components in reptile eggshells results in an interesting variety of material properties such as sorption properties, mechanical performance, antimicrobial protection, water repellency, and UV absorption [3,9,10]. Their ability

* Corresponding author. Ghent University, Department of Biology, Evolution and Optics of Nanostructures Group, Karel Lodewijk Ledeganckstraat 35, Gent, 9000, Belgium.
** Corresponding author. Ghent University, Department of Materials Textiles and Chemical Engineering, Center for Textile Science and Engineering, Tech Lane Science Park 70A, Ghent, 9052, Belgium.
E-mail addresses: Liliana.Dalba@UGent.be (L. D'Alba), Karen.DeClerck@UGent.be (K. De Clerck).

https://doi.org/10.1016/j.mtbio.2025.102032
Received 11 April 2025; Received in revised form 26 June 2025; Accepted 27 June 2025
Available online 27 June 2025

to regulate gaseous sorption is particularly noteworthy, ranging from prominent levels in squamate eggshells to being almost negligible in most crocodile eggshells [8]. By deconstructing reptile eggshells into their individual components and replicating these separate modules, we have developed fully bio-based materials with tunable vapor sorption properties. This modular approach enables customization of performance and offers a sustainable, bio-based alternative to conventional synthetic sorptive materials used in wound dressings, tissue scaffolds, food packaging, and filtration membranes [11–23].

Eggshells are multifunctional bio-composites critical for embryonic protection, gas and water exchange, and mineral provision [3,5,6,24,25]. Unlike avian eggshells, reptile eggshells exhibit remarkable variation in composition and structure, reflecting adaptations to specific breeding environments [3–6,8]. Typically, reptile eggshells consist of a protein-rich fibrous shell membrane overlaid or interspersed with a calcareous component [4,5,10,26,27]. The shell membrane is primarily composed of a fibrous, protein-rich structure, often interwoven with a matrix component that enhances its functionality [5,26,27]. The main protein constituent of the shell membrane is keratin, but the presence of various collagens (types I, V, and X) has also been reported [24,26,28]. The matrix component embedding the proteinaceous fibers is an organic matrix composed of proteins, glycoproteins, and proteoglycans incorporated from the uterine fluid during eggshell formation [26]. Note that, in this study, the term *matrix* refers specifically to all non-fibrous, amorphous protein components in reptile eggshells as well as to the organic matrix added to the biomimetic composites, and does not include the fibrous keratin structure. The fiber density and matrix content of the shell membrane influence the structural support and porosity of the reptile eggshell [3,5,8,24,26,27]. The outer inorganic component primarily consists of calcium carbonate ($CaCO_3$) in its most stable calcite polymorph [5,8,26,29], although the aragonite polymorph is also observed in turtle eggshells [5,29]. The concentration and distribution of $CaCO_3$, which may be compact, diffuse, or entirely absent, vary across species, affecting eggshell flexibility and absorptive properties [3,4,8,10,25,30]. An additional thin cuticle layer, reported in turtles and geckos, and less frequently in snakes and lizards, contributes to water and gas regulation, pathogen defense, and UV protection [4,5,10,26–28,31–34]. While extensively studied in avian eggshells, research on the composition and function of reptilian cuticles remains limited [31]. However, the presence of a lipid component has been reported in avian and squamate cuticles [4,31,34,35].

Water management, essential for embryonic development, is regulated by a balance between environmental absorption and albumen reserves, and is primarily influenced by the eggshells' level of porosity and calcification—which vary greatly across reptile species [3,18,19,22,25,36–40]. Highly calcified eggshells, such as those of crocodiles and turtles, act as water barriers and feature larger albumen volumes, while less calcified, absorptive eggshells, such as those of squamates, enable environmental water uptake [36,40–44]. While our recent study [8] linked water absorption to $CaCO_3$ content using phylogenetic analysis, the interplay between the proteinaceous fibrous membrane, matrix material, and cuticle layer in regulating gaseous exchange and moisture sorption remains underexplored. This work aims to address this knowledge gap by systematically investigating the modular contributions of these components and translating their functional roles into bioinspired materials with tunable properties.

To achieve this, we mimicked four key reptile eggshell components: (1) electrospun keratin nanofibers to replicate the fibrous shell membrane, (2) an organic matrix to serve as the proteinaceous eggshell matrix, (3) $CaCO_3$ particles to introduce mineralization, and (4) a paraffin coating representing the lipid-rich cuticle layer. Solvent electrospinning was previously established as a versatile and scalable method for fabricating keratin-based nanofibrous membranes [45–50]. Upon further optimization of the process, we were able to produce homogeneous and mechanically stable keratin nanofibrous membranes that resemble the fibrous architecture of the inner eggshell layer [2,45,51,52]. These keratin membranes serve as a structural foundation, onto which an egg protein matrix, $CaCO_3$ layer, and paraffin coating were added, enabling controlled layer-by-layer assembly of the composites. This modular design strategy allows for the systematic evaluation of individual and combined contributions of key eggshell components to gaseous sorption behavior, using nanofibrous membranes from extracted keratin for the first time as a biomimetic model.

This modular and bio-based platform not only offers a sustainable alternative to conventional moisture-regulating materials, which often rely on synthetic polymers, fluorinated treatments, or non-degradable additives [13,23,53–56], but also leverages sourcing of keratin from renewable materials—such as poultry feathers, wool, or textiles—for cost-effective and sustainable production [57]. By combining biological origin, biodegradability, and design flexibility, the composites present a promising path toward advanced materials with multifunctional capabilities, inspired by the evolved versatility of reptile eggshells [3,9,10,36,37,39,40].

This research aims to understand the modular contributions of the main eggshell components to water vapor sorption and translate their variability into tunable material properties. Specifically, we hypothesize that (1) the four biomimetic components can effectively replicate the structural modularity of reptile eggshells, (2) the $CaCO_3$ component dominates the sorption properties in the biomimetic composites, effectively reducing gaseous uptake as the mineral content increases, (3) the organic matrix and cuticle layer become more influential in modifying sorption properties when the $CaCO_3$ content is low, and (4) this explains the observed variation in the sorption properties among less calcified eggshells with similar $CaCO_3$ contents. By leveraging a bioinspired and modular design, the framework introduced here provides a sustainable and adaptable solution to challenges in wound dressing development, tissue engineering, packaging materials, filtration processes, and other fields reliant on tunable sorption properties [11–23,56].

2. Material and methods

2.1. Eggshell collection and preparation

Eggs from *Caiman crocodilus* and *Pantherophis guttatus* were donated by the Zoo of Antwerp, while *Python regius* and *Iguana iguana* eggs were acquired from the Pairi Daiza zoo. All eggs were verified to be fresh and free of embryonic development. Following verification, the yolk and albumen were removed, and the eggshells were rinsed with a 70 % ethanol solution. The eggshells were stored at −18 °C until further use. For testing, small fragments were manually cut with a scalpel from the central region of each eggshell, specifically within the middle 50 % of the longitudinal axis, to minimize structural variability. The $CaCO_3$ content of the eggshells was referenced from values reported previously, where we used light microscopy to assess the $CaCO_3$ levels in Alizarin Red-stained eggshell samples [3].

2.2. Keratin extraction

Keratin was extracted from Merino wool through sulfitolysis, following our method outlined in Ref. [58]. The wool was cleaned using Soxhlet extraction to remove fatty matter, followed by thorough washing with distilled water. For extraction, the wool was treated in a urea (8 M, Sigma-Aldrich, reagent grade ≥99.5 %), sodium metabisulfite (0.5 M, Sigma-Aldrich, reagent grade ≥99 %) solution under continuous shaking at 60 °C for 2.5 h. The pH of this solution was adjusted to 6.5 using sodium hydroxide (5 M, Carlo Erba, reagent grade ≥97 %). The obtained keratin solution was filtered and dialyzed against distilled water in a cellulose dialysis tube with a molecular cut-off of 12,000–14,000. The final keratin solution was freeze-dried into a keratin powder, which was stored under vacuum until further use (within 1 month).

2.3. Keratin electrospinning

Electrospinning solutions were prepared by dissolving 17 wt% extracted keratin in formic acid (Sigma-Aldrich, reagent grade ≥98 %) at room temperature under constant stirring. The solutions were electrospun using a horizontal dual-needle setup (Inner diameter needle: 0.25 mm) with a centralized rotating drum collector (Length: 12 cm; Outer diameter: 3 cm), wrapped in aluminum foil to facilitate membrane removal (Fig. 2E). Electrospinning was performed at a constant flow rate of 0.20 ml h^{-1} (KD Scientific Syringe Pump, Series 100), a tip-to-collector distance of 15 cm, and a positive voltage of 25 kV (Glassman High Voltage Series, EH-b voltage source). These parameters yielded stable and continuous nanofiber production. To enhance water stability, the resulting keratin membranes were thermally treated at 180 °C for 2 h [59]. The resulting membranes were stored in a climatized laboratory environment (23 ± 1 °C; 25 ± 2 % RH) until further use. Two different keratin membranes, labeled A and B, were prepared from different extraction batches but following the same sulfitolysis procedure. Estimated protein secondary structure contributions of the keratin membranes were based on our previous work in Ref. [45] and obtained through FTIR deconvolution analysis. The results are provided in the *Supporting Information* (Supplementary Table 1).

2.4. Biomimicry of the matrix module

To imitate the eggshell's organic matrix, the keratin membranes were dip-coated in aqueous solutions of egg protein powder (chicken egg white powder, Sigma-Aldrich) with concentrations of 0.5 wt%, 1.0 wt%, and 5.0 wt% (Fig. 1A; Supplementary Table 2). Keratin membranes, supported by aluminum foil, were submerged in these solutions for 3 h under continuous ultrasonic stirring. After dip-coating, the membranes were dried at room temperature and removed from the aluminum support.

2.5. Biomimicry of the mineral module

$CaCO_3$ powder (Sigma-Aldrich, reagent grade ≥99.0 %) was used to mimic the mineral component of reptile eggshells. The powder was confirmed to be in the calcite polymorph via X-ray diffraction (XRD) analysis (Supplementary Fig. 1A). Particle size analysis based on SEM images (ImageJ software, n = 100) revealed a size distribution of 1–100 μm (Supplementary Fig. 1B). The powder was manually deposited on top of the keratin membranes and gently leveled with a scalpel to form composites with keratin – to – $CaCO_3$ ratios of 90/10, 50/50, and 10/90, determined by weight (Fig. 1B; Supplementary Table 2). The layers were physically assembled without chemical bonding, using gravity to maintain the structure during handling and measurements.

2.6. Biomimicry of the lipid module

The lipid component, typically present in the cuticle layer of reptile eggshells, was mimicked by dip-coating the keratin membranes in paraffin (melting temperature of 50–52 °C; Carl Roth) solutions. Homogeneous paraffin solutions with concentrations of 0.5 wt%, 1.0 wt%, and 5.0 wt% were prepared in ethanol (VWR Chemicals®, analytical reagent ≥99.8 %) at 80 °C (Fig. 1C; Supplementary Table 2). Keratin membranes, supported by aluminum foil, were dipped in these solutions for 1 min and dried at room temperature, after which the aluminum foil

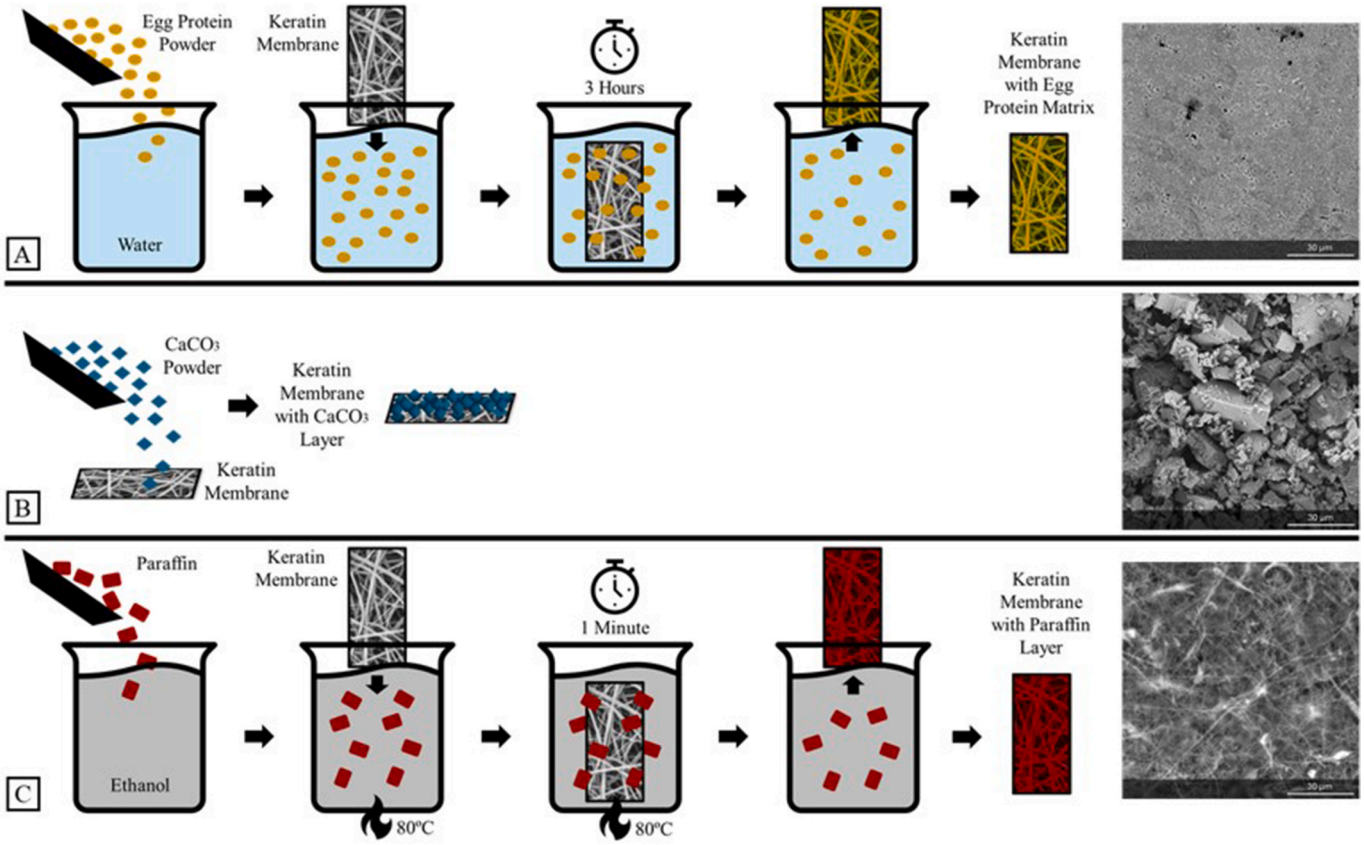

Fig. 1. Schematic overview of the modular fabrication methods of all investigated keratin-based composites. (A) Dip-coating process of keratin membranes in egg protein solutions to mimic the eggshell's matrix component, with top-view SEM image of a keratin–matrix composite membrane (~65 % egg protein). (B) $CaCO_3$ deposition onto keratin membranes to mimic the eggshell's mineralized layer, with top-view SEM image of a keratin–$CaCO_3$ composite membrane (10/90 weight ratio). (C) Dip-coating process of keratin membranes in paraffin solutions to mimic the eggshell's lipid component, with top-view SEM image of a keratin–paraffin composite membrane (~65 % paraffin). A full list of sample compositions is provided in Supplementary Table 2.

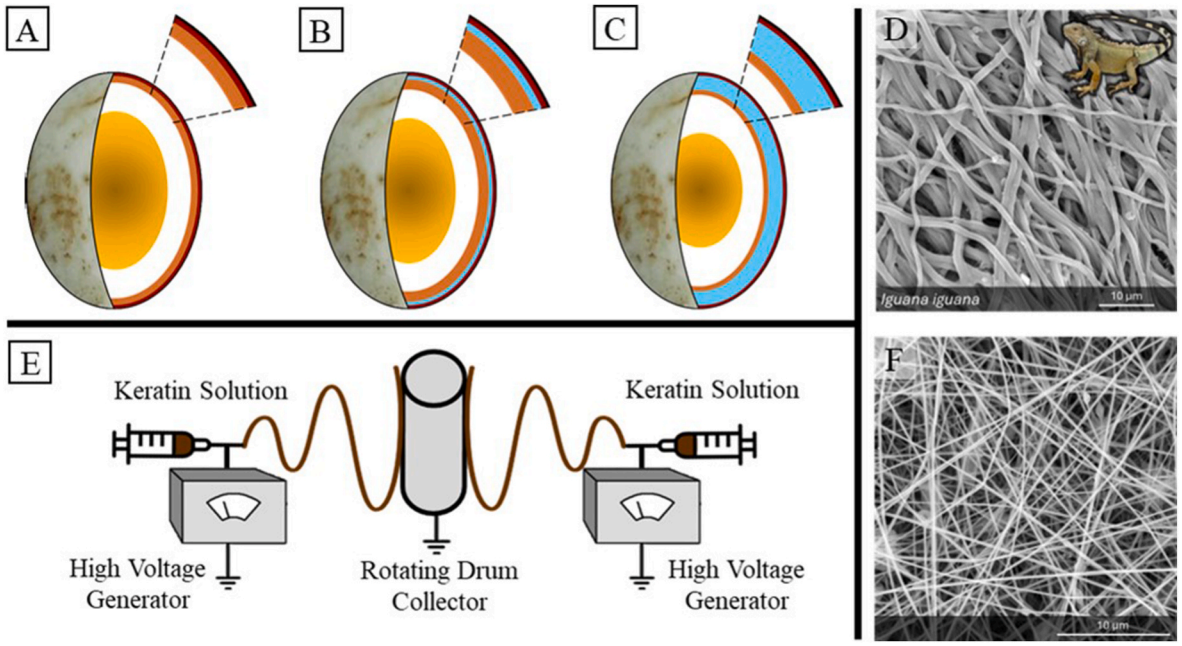

Fig. 2. Schematic illustration of the general modular composition of reptile eggshells (Orange – proteinaceous, fibrous membrane with or without organic matrix; Blue – $CaCO_3$ component; Red – cuticle layer): (A) eggshell without $CaCO_3$ component, (B) eggshell with a thin $CaCO_3$ layer, and (C) eggshell with a thick $CaCO_3$ layer. (D) Top-view SEM image of the proteinaceous, fibrous membrane of *Iguana iguana*. (E) Schematic illustration of the horizontal dual-needle electrospinning setup with centralized rotating drum collector, used for SES of extracted keratin. (F) Top-view SEM image of keratin membrane A. (For interpretation of the references to color in this figure legend, the reader is referred to the Web version of this article.)

was removed.

2.7. Scanning Electron Microscopy

A Phenom XL Desktop Scanning Electron Microscope (Thermo Fisher Scientific) was used to visualize the modularity of the reptile eggshells and to analyze the biomimetic composites. Imaging was performed at accelerating voltages of 10–15 kV using a backscattered-electron detector. Before analysis, all samples were sputter-coated with a 10–12 nm layer of gold particles using a Plasmatool-SC sputter coater. Cross-sectional SEM samples were prepared by cutting both eggshell and biomimetic samples after submersion in liquid nitrogen.

SEM images were used to evaluate the morphology of the electrospun keratin membranes. Nanofiber diameters were measured using ImageJ software ($n = 100$) and determined as 251 ± 44 nm and 286 ± 49 nm for keratin membrane A and B, respectively. To estimate the mean pore diameter and pore height of the electrospun membranes, we applied the analytical approach described by Eichhorn et al. (2010) [60], which correlates nanofiber diameter and membrane density to calculate the pore dimensions in nanofibrous membranes. The resulting values for keratin membrane A and B are provided in Supplementary Table 3.

2.8. Thermogravimetric Analysis

Thermogravimetric Analysis (TGA) (Mettler Toledo, TGA 2) was conducted to estimate the percentage of egg protein and paraffin in the biomimetic models (Supplementary Fig. 2; Supplementary Table 4). The samples were heated from 25 °C to 600 °C at 10 °C min^{-1} under a nitrogen atmosphere. The egg protein content was calculated based on the mass loss at 600 °C, comparing the egg protein composite samples to pure egg protein and keratin membrane A. Similarly, the paraffin content was determined by comparing the mass loss at 121 °C in the paraffin composite samples to pure paraffin and keratin membrane B.

2.9. Fourier-Transform Infrared Spectroscopy

Infrared absorption spectra of the reptile eggshells and biomimetic components were obtained using a Fourier Transform Infrared (FTIR) spectrometer (Nicolet™ iS50, Thermo Scientific) equipped with an Attenuated Total Reflectance (ATR) module. The samples were excited using light with wavenumbers ranging from 4000 to 400 cm^{-1}, with a resolution of 4 cm^{-1} and 32 scans per measurement. Baselines were corrected using Origin 8.5 (Peak Analyzer) and spectra were normalized to their maximum peak.

2.10. Dynamic Vapor Sorption

The water vapor sorption of the reptile eggshells and biomimetic models was measured using a Q5000-SA Dynamic Vapor Sorption (DVS) apparatus from TA instruments. Samples of 2.50 ± 0.50 mg were placed in metallized quartz pans. Following a drying step at 60 °C and 0 % relative humidity (RH), the relative humidity was increased and subsequently decreased in steps of 15 %, from 5 % RH to 95 % RH, at a constant temperature of 23 °C. Equilibrium was defined as a mass change <0.05 % during 45 min. Sorption isotherms were generated based on the average results of 1–3 measurements, with error bars representing the standard deviation when multiple measurements were performed. For *Caiman crocodilus*, DVS measurements were conducted on the distinct inner and outer eggshell layer, which were separated and gently wiped with a cotton swab to remove residue from the adjoining surface.

3. Results and discussion

3.1. Biomimicry of reptile eggshell modularity

This study focused on replicating the structural and functional modularity of reptile eggshells (Fig. 2A–C) to develop biomimetic composites with tunable water vapor sorption properties. Therefore, four primary eggshell components—proteinaceous fibrous membrane,

organic matrix, $CaCO_3$ component, and cuticle layer—were reconstructed using electrospun keratin membranes, egg protein powder, $CaCO_3$ powder, and paraffin, respectively. The biomimetic components were analyzed using Scanning Electron Microscopy (SEM) and Fourier-Transform Infrared (FTIR) spectroscopy.

The fibrous shell membrane of reptile eggshells (Fig. 2D) shares structural similarities with nanofibrous membranes produced via solvent electrospinning (SES) (Fig. 2F). For instance, fiber diameters of 1.0 ± 0.2 μm were measured for *Iguana iguana* eggshells (Fig. 2D) and reported fiber diameters for various other reptile eggshells range from 0.2 to 4.0 μm [3,61]. To mimic this structure, keratin extracted from Merino wool via sulphitolysis was electrospun using a horizontal dual-needle setup (Fig. 2E). Electrospinning of keratin offers a scalable approach for fabricating fibrous scaffolds with tunable porosity and structural control, resulting in membranes that resemble the fibrous morphology observed in reptile eggshell shell membranes [2,45,51,52].The resulting keratin membranes, A and B, exhibited average fiber diameters of 251 ± 44 nm and 286 ± 49 nm, respectively (Fig. 2F; Supplementary Fig. 3; Supplementary Table 3). Beyond this achievement, the technique also enables the design of more diverse fiber architectures found in eggshells, such as aligned nanofibrous membranes or layered keratin sheets with controlled nanofiber orientations [51,52,62].

The electrospun keratin membranes were functionalized with an organic matrix to mimic the protein-rich component embedding the fibrous shell layer in reptile eggshells (Fig. 1A). Dip-coating in aqueous solutions of dried chicken egg white powder, which contains proteins such as ovalbumin, lysozyme, and ovotransferrin—analogous to reptilian "egg white" proteins [26,28]—resulted in membranes with ~20 %, ~30 %, and ~65 % egg protein by weight (Fig. 1A; Supplementary Fig. 4). The egg protein content was quantified using Thermogravimetric Analysis (TGA) (Supplementary Fig. 2; Supplementary Table 4).

To model the calcareous component, a thick outer layer composed of $CaCO_3$ in its calcite polymorph [5,26,29] was deposited onto the keratin membranes (Fig. 1B; Supplementary Fig. 1). While this approach does not result in a chemically bonded or structurally integrated mineral phase, it enabled modular investigation of the influence of the mineral component on water vapor sorption.

The reptilian cuticle, although not fully characterized to date, is known to contain a lipid constituent [4,31,34,35]. Paraffin, due to its simple hydrocarbon-based nature, was selected as an initial biomimetic substitute for this component and applied to the keratin membranes via dip-coating in varying concentrations (~15 %, ~20 %, and ~65 % by weight; Fig. 1C; Supplementary Fig. 5). Future studies will involve an in-depth investigation of the reptilian cuticle layer to aid in the selection of more biologically relevant lipid analogues and the replication of the cuticle microstructure to accurately mimic its surface topography [31, 34].

By systematically combining the organic matrix, mineral layer, and lipid coating with the keratin membranes in varying concentrations, a diverse range of biomimetic architectures was obtained. Fig. 3 presents cross-sectional SEM images of representative composites developed in this study, alongside the reptile eggshells that served as their biological templates (Supplementary Fig. 6).

Python regius and *Iguana iguana* eggshells (Fig. 3D and E) are mainly composed of proteinaceous fibers, with a negligible amount of matrix material and low $CaCO_3$ content (6 % and 1.5 %, respectively). The nanofibrous structure of the biomimetic keratin membranes (Top-view: Fig. 2F, Cross-sectional view: Fig. 3A) captures the general fibrous microstructure observed in these eggshells (Top-view: Fig. 2D, Cross-sectional view: Fig. 3D and E). While some structural differences are observed—such as heterogeneity in fiber morphology and fiber clustering, which are not present in the uniformly distributed keratin nanofibers—this work aims to reproduce the modular composition and functionality of the eggshells in view of mimicking their water vapor sorption properties, rather than their exact microstructural arrangement. The uniformity and homogeneity of the electrospun fibers—while differing from the natural heterogeneity seen in reptile eggshells—are,

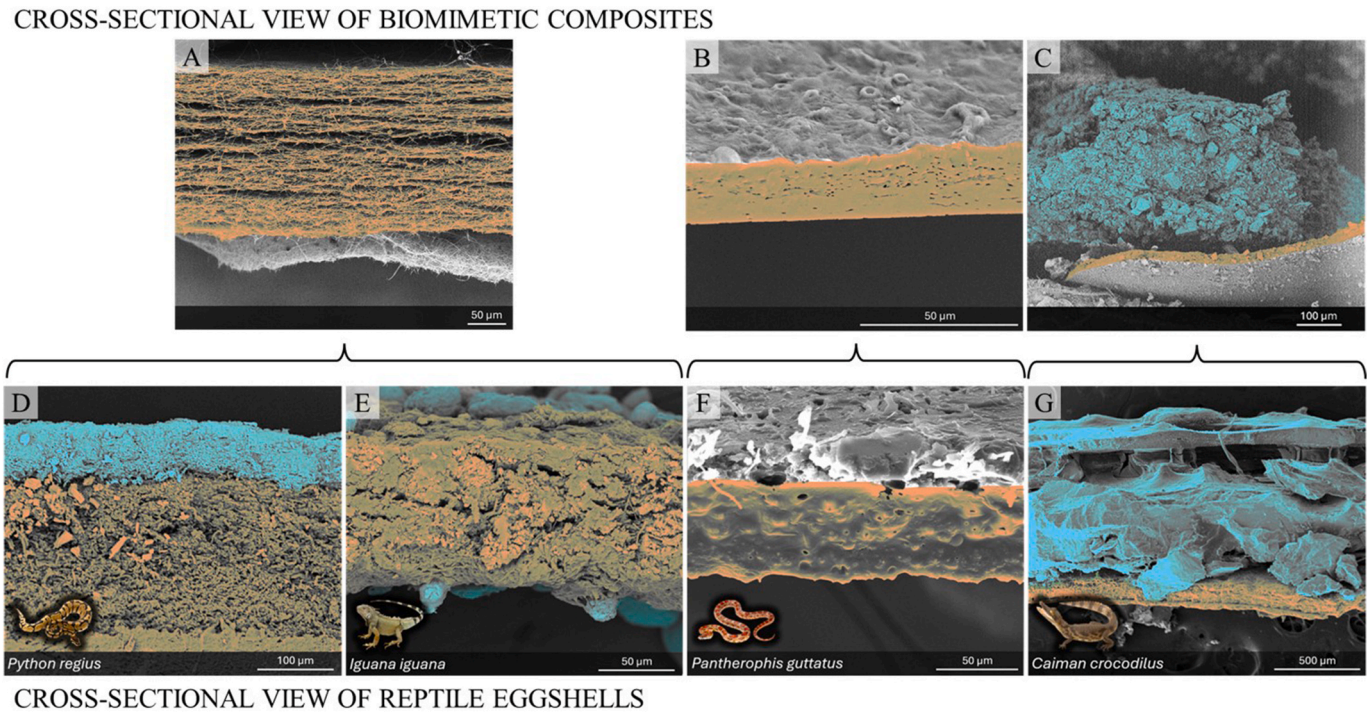

Fig. 3. Cross-sectional SEM images of biomimetic composites and the reptile eggshells that served as their reference (oriented with their outer surface at the top). (A) Keratin membrane B vs. (D) Python regius and (E) *Iguana iguana*; (B) Keratin membrane A enriched with egg protein matrix vs. (F) *Pantherophis guttatus*; (C) Keratin membrane B with $CaCO_3$ layer vs. (G) *Caiman crocodilus*. Color overlays: Orange – proteinaceous, fibrous membrane with or without organic matrix; Blue – $CaCO_3$ component. (For interpretation of the references to color in this figure legend, the reader is referred to the Web version of this article.)

in fact, advantageous for membrane applications, as this reduces local variability in material performance and improves reproducibility and reliability.

In contrast, the *Pantherophis guttatus* eggshell (Fig. 3F), which features a substantial amount of organic matrix, served as a reference for developing keratin membranes enriched with an egg protein matrix (Fig. 3B). The addition of this matrix increased the membrane's structural density, thereby successfully mirroring the composite character of

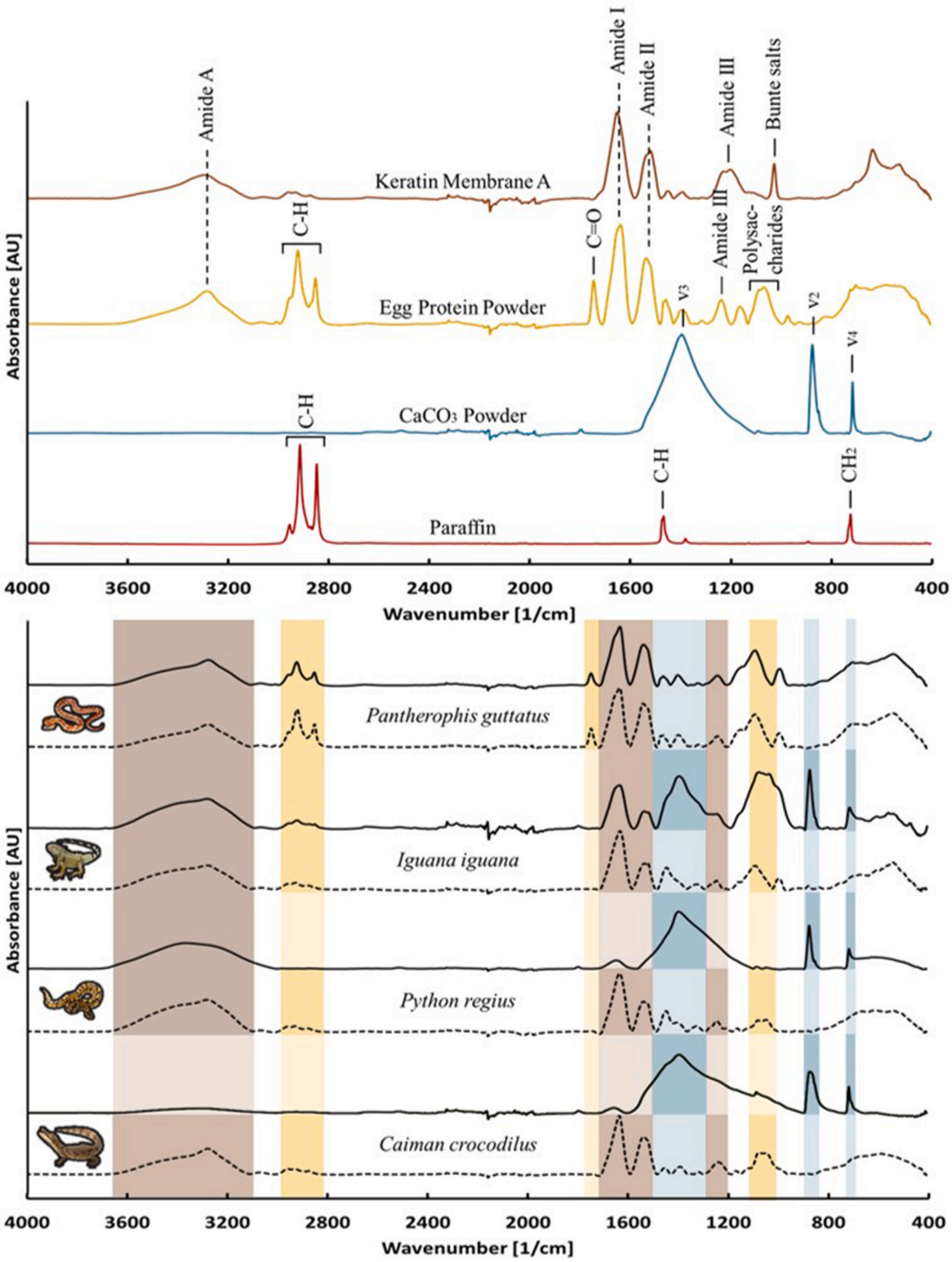

Fig. 4. Top – FTIR spectra of the biomimetic modules: keratin membrane A, egg protein powder, $CaCO_3$ powder, and paraffin, with characteristic absorption peaks and bands indicated. Bottom – FTIR spectra of the outer surface (solid line) and inner surface (dotted line) of *Pantherophis guttatus*, *Iguana iguana*, *Python regius*, and *Caiman crocodilus* eggshells, with important absorption peaks and bands highlighted. Band colors correspond to the spectra colors of the biomimetic modules. [AU] Arbitrary units. (For interpretation of the references to color in this figure legend, the reader is referred to the Web version of this article.)

the natural reptile eggshell.

A highly mineralized eggshell, such as that of *Caiman crocodilus* (Fig. 3G), which contains approximately 90 % $CaCO_3$, was used as a reference for developing mineralized keratin composites (Fig. 3C). Depositing $CaCO_3$ powder onto the keratin membranes yielded a modular composite that captures the key compositional features of its natural counterpart and enabled the study of sorption behavior in highly calcified systems. Nevertheless, future studies will explore advanced strategies to more closely replicate the mineral microstructure in reptile eggshells as to understand its possible relation to performance. This includes controlled biomineralization as the mineral layer in reptile eggshells is known to grow directly from the proteinaceous layer [5,28,63–65].

In summary, the developed biomimetic models effectively replicate the modular nature of reptile eggshells, demonstrating their potential for tunability and application-driven material engineering using bio-based materials. A future research direction includes the production of keratin-based composites combining all four biomimetic components (keratin, matrix, $CaCO_3$ and lipid) and varying their respective concentrations to further increase the structural and functional diversity.

3.2. Chemical analysis of the biomimetic composites

Fourier-Transform Infrared (FTIR) spectroscopy was used to analyze the individual biomimetic modules and compare their chemical composition to representative reptile eggshells, assessing their biomimetic resemblance.

The FTIR spectra of the keratin membranes (Fig. 4, Top; Supplementary Fig. 3), designed to mimic the proteinaceous shell membrane, display characteristic amide vibration modes. The broad absorption band around 3300 cm^{-1} is related to amide A groups, specifically the stretching vibrations of N–H bonds and O–H bonds [32,45,47,66]. The C=O stretching vibrations of Amide I are observed around 1650 cm^{-1} [45,47,66]. Amide III and Amide IV are mixed vibrational modes. Amide III arises from the out-of-phase combination of in-plane N–H bending and C–N stretching vibrations (1540–1510 cm^{-1}), while Amide IV results from the in-phase combination of N–H in-plane bending and C–N stretching vibrations, with minor contributions from C–C stretching and C=O bending vibrations (1250–1200 cm^{-1}) [45,47,66]. These features closely match the FTIR spectra of the eggshell surfaces of *Iguana iguana* (inner and outer), *Python regius* (inner), and *Caiman crocodilus* (inner) (Fig. 4, Bottom), confirming the predominantly keratinous nature of the natural shell membranes. However, minor contributions from other structural proteins, such as collagens [24,26,28], may be present in eggshell membranes. Notably, the dual needle SES setup (Fig. 2E) used in this study enables co-electrospinning of multiple proteinaceous components, such as keratin and collagen, which could further enhance the chemical accuracy of the biomimetic model [24,46]. Furthermore, the absorption peak at 1024 cm^{-1} on the FTIR spectra of the keratin membranes (Fig. 4, Top) corresponds to the symmetric S–O stretching vibrations of Bunte salt residues from the keratin sulfitolysis extraction process [45,47].

The egg protein powder (Fig. 4, Top), used to enrich the biomimetic composites with an organic matrix, also exhibits the amide vibration modes. These peaks are supplemented by particularly strong C–H bending and stretching vibration peaks (2950–2850 cm^{-1}) [67,68]. The absorption peak at 1744 cm^{-1} is attributed to the stretching vibrations of C=O groups [8,69]. The FTIR peak around 1460 cm^{-1} is associated with carboxylate groups from amino acid residues [32], and bending vibrations of methyl groups [70]. Symmetric carbon-hydrogen bending vibrations of CH_3 groups appear at 1385 cm^{-1} [67,68], while the peak at 1160 cm^{-1} corresponds to C–H bonds [8]. The broad band around 1100–990 cm^{-1} is linked to the C–O stretching modes of polysaccharides [32,34] and the absorption peak at 970 cm^{-1} suggests the presence of phosphate groups [8,34,70]. These features align with the FTIR spectra of the matrix-rich *Pantherophis guttatus* eggshell (Fig. 4, Bottom), supporting the validity of this module in mimicking the organic matrix. However, natural variations in protein composition among reptile eggshells suggest that fine-tuning the blend of matrix proteins could further improve biomimetic accuracy [26,28].

$CaCO_3$ powder (Fig. 4, Top), representing the mineral layer, exhibits characteristic calcite absorption bands at 1393 cm^{-1} (ν_3), 872 cm^{-1} (ν_2), and 712 cm^{-1} (ν_4) [64,71–73], closely aligning with the FTIR spectra of the outer eggshell surfaces of *Caiman crocodilus* and *Python regius* (Fig. 4, Bottom). Furthermore, the modular nature of this model allows for additional refinement to expand its versatility. For instance, alternative $CaCO_3$ polymorphs, such as aragonite—found in some turtle eggshells [5,29]—or a dispersed mineral phase grown directly from the keratin nanofibers [5,28,63–65], could enable biomimetic resemblance to a broader range of natural eggshells. These possibilities reinforce the adaptability of this biomimetic platform in replicating diverse eggshell compositions and structures.

The paraffin coating (Fig. 4, Top), included to represent the lipid constituent of the reptilian cuticle, exhibits characteristic C–H stretching (2950–2850 cm^{-1}), C–H deformation or bending vibration (1470 cm^{-1}), and CH_2 rocking absorption (720 cm^{-1}) [67,68]. However, these peaks are not distinctly observed in the FTIR spectra of the investigated reptile eggshells, which lack a well-defined cuticle, as confirmed by SEM analysis (Fig. 3D–G). Since the precise composition and concentration of reptilian eggshell cuticles remain poorly understood [31], refining the biomimetic model of this component will require further investigation into its chemical profile and functional role. Nevertheless, with its simple hydrocarbon backbone, paraffin serves as an initial, chemically relevant, analogue for the lipid component in the cuticle, providing a reliable model to assess the impact of the lipid-containing layer on the sorption properties of reptile eggshells.

3.3. Analysis of gaseous sorption behavior of the biomimetic composites

We previously reported the vapor sorption properties of 62 reptile eggshells [8]. Fig. 5 illustrates their sorption profiles as determined by Dynamic Vapor Sorption (DVS), color-coded to emphasize the effect of the $CaCO_3$ content on their sorption properties. The 22 eggshells with less than 10 % $CaCO_3$ exhibit gaseous absorption ranging from 15 % to 42 %, whereas the 6 eggshells with over 90 % $CaCO_3$ display a much narrower absorption range of 1–4 % (Fig. 5). Thus, although the $CaCO_3$ component is the dominant factor controlling the vapor sorption properties in highly calcified eggshells, significant variation is still observed among eggshells with lower $CaCO_3$ contents, suggesting that additional chemical or structural factors influence their sorption behavior. To

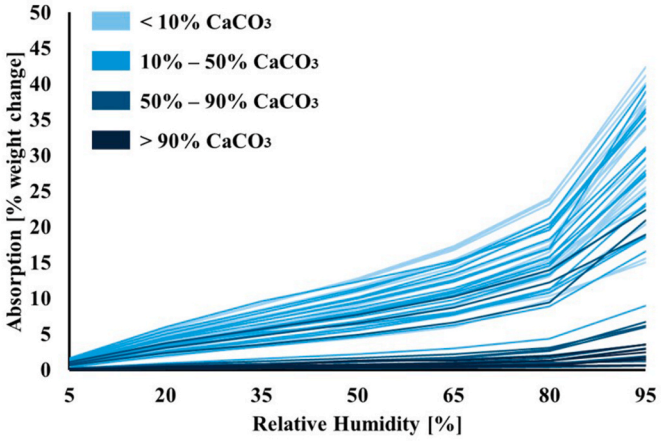

Fig. 5. Absorption profiles of 62 reptile eggshells, measured from 5 % RH to 95 % RH (at 25 °C), with color-coding to indicate their $CaCO_3$ content. Adapted from Ref. [8]. (For interpretation of the references to color in this figure legend, the reader is referred to the Web version of this article.)

explore this, we investigated the contributions of the key eggshell components—namely the proteinaceous fibrous layer, organic matrix, $CaCO_3$ component, and lipid coating—using the previously described biomimetic models.

As a first step, the vapor sorption behavior of the pure biomimetic modules—keratin membranes A and B, egg protein powder, $CaCO_3$ powder, and paraffin—was investigated (Fig. 6A). The keratin membranes and egg protein powder show high absorption values of 44 ± 0.7 %, 33 ± 1.2 %, and 35 ± 0.2 % at 95 % RH, respectively (Fig. 6A; Supplementary Table 5). The difference in gaseous absorption between pure keratin membrane A (44 ± 0.7 % at 95 % RH) and B (33 ± 1.2 % at 95 % RH) highlights how small variations in composition and structure can significantly influence the gas exchange properties. These differences may arise from minor variations in keratin batch composition, protein folding, or possible aging effects (Supplementary Table 1) [45,59,74,75]. Additionally, morphological differences in the nanofibrous membranes, such as nanofiber diameter or porosity, may contribute to the observed variation in gaseous sorption (Supplementary Table 3). Both the molecular and morphological characteristics of the electrospun keratin membranes can be modulated by tuning the electrospinning parameters, including the solvent system, applied voltage, tip-to-collector distance, flow rate, and collector rotation speed [45,51,52]. This tunability represents a first step toward replicating the nuanced permeability variations observed in reptile eggshells and demonstrates the potential of electrospun keratin membranes for applications requiring tunable vapor sorption behavior [2,51,52].

The absorption isotherms of the keratin membranes and egg protein powder are classified as Type III by IUPAC, characteristic of macroporous and non-porous absorbents with strong absorbate-absorbent interactions [76,77]. This behavior aligns with the large molar weight, considerable number of polar groups, and numerous potential hydrogen bonding sites in protein and peptide structures, which promote strong interactions with water molecules [74,77]. Significant water vapor absorption/desorption hysteresis was observed for the keratin membranes compared to the other biomimetic modules (Supplementary Fig. 7; Supplementary Table 5; Supplementary Table 6). Classified as type H-3 loops by IUPAC, this hysteresis is typically associated with irreversible covalent sorbate binding, capillary condensation in pores, slow equilibration, or structural relaxation of the sorbent [74,76]. SEM images revealed morphological changes in the keratin membranes after the DVS measurements, supporting the hypothesis that structural relaxation is the primary mechanism underlying the observed hysteresis (Supplementary Fig. 8).

In contrast to the proteinaceous modules, $CaCO_3$ exhibits a very low absorption of 0.2 ± 0.03 % at 95 % RH (Fig. 6A; Supplementary Table 5), consistent with reptile eggshells containing over 90 % of $CaCO_3$ (Fig. 5). This is consistent with its crystalline, inorganic structure, which limits the number of available sites for sorption [78]. Similarly, paraffin displays low absorption of 0.2 ± 0.02 % at 95 % RH (Fig. 6A; Supplementary Table 5), which can be attributed to the absence of absorption sites on its hydrocarbon backbone [79]. The absorption isotherms of both $CaCO_3$ and paraffin are classified as Type II by IUPAC, representing absorption on macroporous and non-porous absorbents with weak absorbate-absorbent interactions [76].

To examine the influence of the $CaCO_3$ content on the overall sorption properties, varying amounts of $CaCO_3$ (10 %, 50 %, and 90 % by

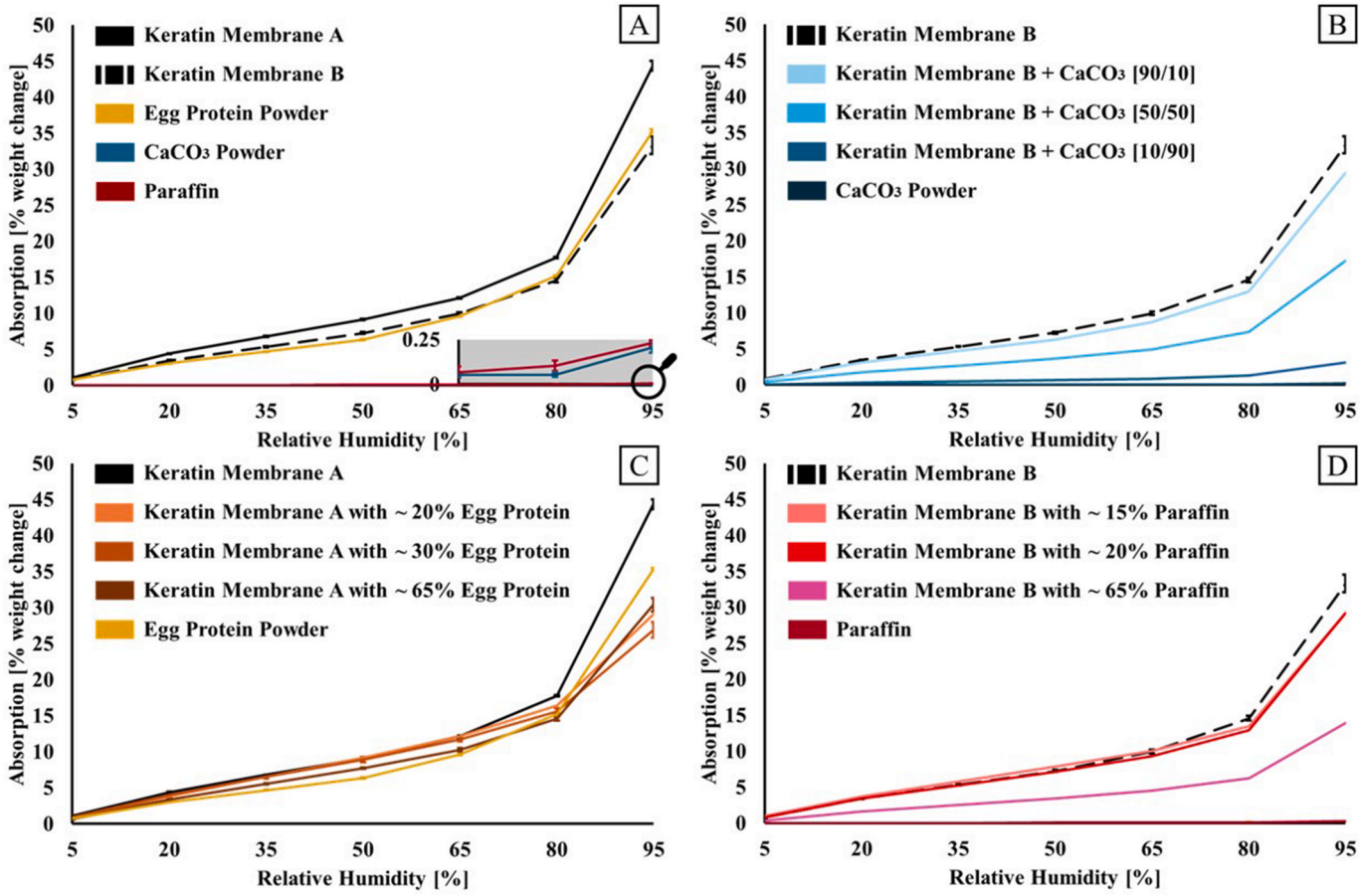

Fig. 6. Absorption profiles measured from 5 % RH to 95 % RH (at 23 °C) for (A) pure biomimetic modules, including a zoomed-in view from 65 % RH to 95 % RH for $CaCO_3$ powder and paraffin, (B) combinations of keratin membrane B with varying amounts of $CaCO_3$ (10 %, 50 %, and 90 % by weight), (C) combinations of keratin membrane A with varying amounts of egg protein (~20 %, ~30 %, and ~65 % by weight, as estimated using TGA results), and (D) combinations of keratin membrane B with varying amounts of paraffin (~15 %, ~20 %, and ~65 % by weight, as estimated using TGA results).

weight) were layered onto keratin membrane B (Fig. 6B). As hypothesized, the full range from high to low absorption values—29 % for 10 % $CaCO_3$, 17 % for 50 % $CaCO_3$, and 3.1 % for 90 % $CaCO_3$ at 95 % RH—could be achieved by varying the $CaCO_3$ content (Supplementary Table 5), demonstrating a tunable sorption response.

Subsequently, the effect of incorporating an organic matrix was examined (Fig. 6C). Since both the egg protein matrix and the keratin membranes are protein-based, they share general chemical characteristics such as polar functional groups and hydrophilic domains. This underlies the comparable absorption isotherms observed at low to moderate relative humidity (up to 65 % RH). In this range, the composite samples show intermediate moisture uptake, with increasing egg protein content shifting the sorption profile toward that of the egg protein. However, above 65 % RH, moisture uptake in the composites declines relative to the pure egg protein. This behavior likely arises from the reduced pore volume and restricted diffusion pathways caused by matrix integration, which may hinder water vapor penetration [74,76,77].

Finally, the influence of a lipid component was assessed by integrating a paraffin coating onto keratin membrane B (Fig. 6D). Due to the stark contrast in vapor absorption between the pure keratin membrane and paraffin, variation of the paraffin concentration allows for substantial modulation of sorption properties. Absorption reductions range from approximately 4 % for ~15 % paraffin addition to around 19 % for ~65 % paraffin addition. However, the substantial reduction in absorption observed in the composite containing ~65 % paraffin does not match the maximal sorption decrease observed in reptile eggshells with limited $CaCO_3$ content. This discrepancy likely stems from the relatively low lipid concentration in reptilian cuticles, which has been reported as very low to negligible in some squamates [31] and around 3 % in chicken eggshells [31,32,80].

The influence of adding $CaCO_3$ and matrix components to the keratin-based fibrous membranes was further evaluated by comparing the sorption behavior of the composite biomimetic models to the eggshells of *Caiman crocodilus* and *Pantherophis guttatus* (Fig. 7). The *Caiman crocodilus* eggshell represents a reptile eggshell with a proteinaceous fibrous membrane containing a low matrix concentration and approximately 90 % $CaCO_3$ (Fig. 7B and C). The vapor sorption of this eggshell was compared to that of the biomimetic model containing 10 % keratin membrane B and 90 % $CaCO_3$ by weight (Fig. 7A). The maximum absorption value of the biomimetic model, 3.1 %, aligns closely with the maximum absorption value of 5.1 ± 0.3 % observed for the *Caiman crocodilus* eggshell (Supplementary Table 5). To further analyze the contributions of individual eggshell components, the *Caiman crocodilus* inner proteinaceous membrane and outer calcareous layer were examined separately using DVS analysis (Fig. 7A). The inner membrane exhibits an absorption value of 44 ± 1.4 % at 95 % RH, while the outer layer has a much lower absorption value of 1.4 ± 0.3 % at 95 % RH (Supplementary Table 5). These values correspond well to those of the respective biomimetic modules: 33 ± 1.2 % for keratin membrane B and 0.2 ± 0.03 % for $CaCO_3$ (Supplementary Table 5). It should be noted that, in contrast to the natural mineral component in reptile eggshells—where the $CaCO_3$ is grown directly from the underlying fibrous layer via biomineralization [25,28,63]—our $CaCO_3$ component was deposited as a discrete surface layer composed of calcite particles. Future work will explore advanced strategies to more closely replicate the mineral microstructure in reptile eggshells as to understand its possible relation to performance.

The *Pantherophis guttatus* eggshell, which contains a high organic matrix content, was used as a reference for evaluating the sorption behavior of the biomimetic composite model of a keratin membrane embedded in an egg protein matrix (Fig. 7E and F). The absorption isotherm of the eggshell aligns almost perfectly with that of the biomimetic model containing ~65 % egg protein up to 80 % RH (Fig. 7D). At relative humidity above 80 %, the model's absorption values start to diverge, likely due to differences in chemical or structural composition

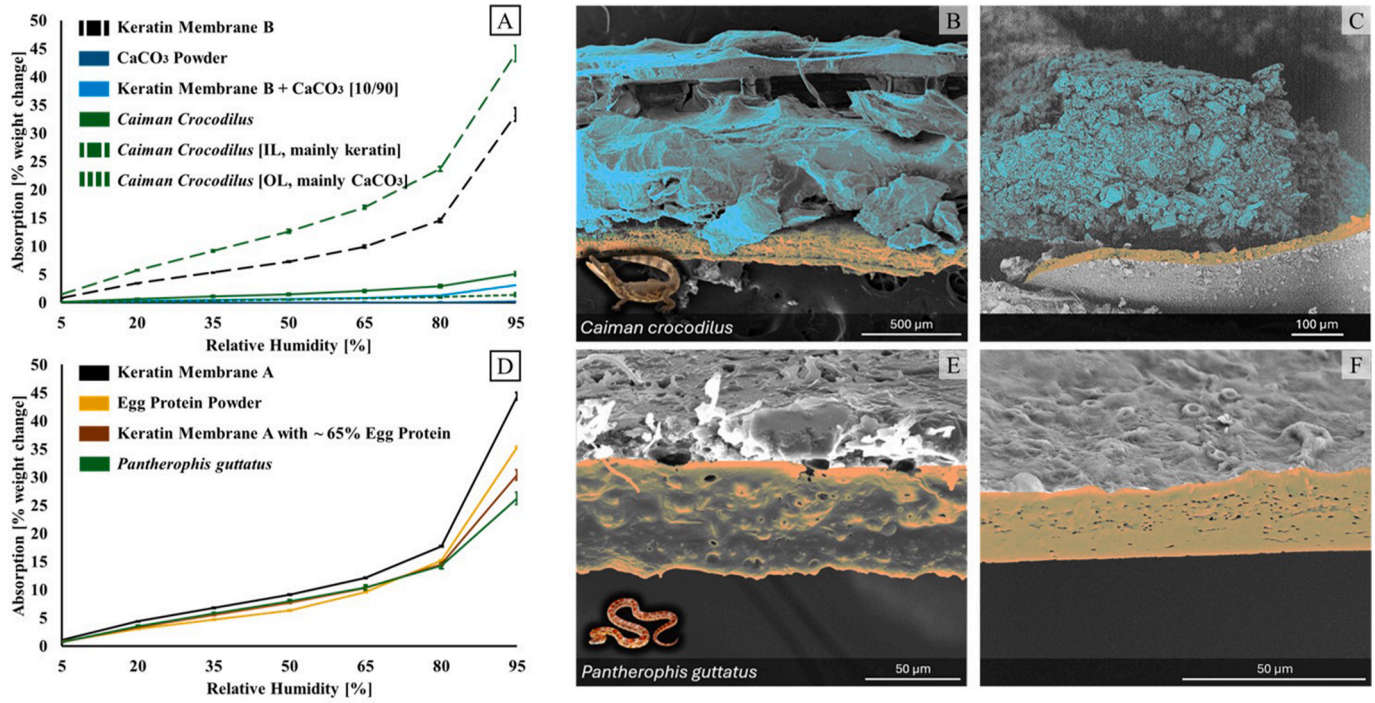

Fig. 7. (A) Absorption profiles measured from 5 % RH to 95 % RH (at 23 °C) for the *Caiman crocodilus* eggshell, its inner layer (IL), and its outer layer (OL), compared to the biomimetic model consisting of keratin membrane B with $CaCO_3$ in a 10/90 weight ratio. (B) Cross-sectional SEM image of the *Caiman crocodilus* eggshell oriented with its outer surface at the top. (C) Cross-sectional SEM image of the biomimetic approximation of the *Caiman crocodilus* eggshell i.e., keratin membrane A with $CaCO_3$ layer. (D) Absorption profiles measured from 5 % RH to 95 % RH (at 23 °C) for the *Pantherophis guttatus* eggshell, compared to the biomimetic model consisting of keratin membrane A with ~65 % egg protein. (E) Cross-sectional SEM image of the *Pantherophis guttatus* eggshell, oriented with its outer surface at the top. (F) Cross-sectional SEM image of the biomimetic approximation of the *Pantherophis guttatus* eggshell i.e., keratin membrane B with egg protein matrix.

arising from the model's simplified design [76].

Finally, absorption/desorption hysteresis of the biomimetic composites corresponds well to that of the examined reptile eggshells (Supplementary Fig. 7; Supplementary Table 5; Supplementary Table 6), further validating the accuracy of the moisture sorption behavior of the models.

The DVS results support the hypothesis that the $CaCO_3$ component predominantly governs vapor sorption properties, acting as an effective barrier against environmental moisture uptake. Highly mineralized reptile eggshells, such as those of *Caiman crocodilus* (89 % $CaCO_3$) (Fig. 5; Fig. 7A), exhibit minimal vapor absorption (<5 %), relying primarily on their albumen as a water source for embryonic development [40–42]. This trend is accurately replicated in the biomimetic keratin–$CaCO_3$ composites, where increasing the $CaCO_3$ content from 10 % to 90 % results in a proportional decrease in vapor sorption (Fig. 6B), fully encompassing the range observed in natural eggshells (Fig. 5).

In contrast, weakly calcified eggshells exhibit higher permeability, allowing greater water vapor passage through their porous structure [36,40,42]. However, considerable variation in vapor absorption is also observed among weakly calcified reptile eggshells with similar $CaCO_3$ contents. For instance, at 95 % RH, absorption ranges from ~15 % in *Xerotyphlops vermicularis* (0.5 % $CaCO_3$) and *Scincus scincus* (29 % $CaCO_3$) eggshells to ~40 % in *Iguana iguana* (1.5 % $CaCO_3$) and *Varanus griseus* (15 % $CaCO_3$) eggshells (Fig. 5). This variation can be explained by differences in matrix content or the presence of a cuticle layer [8]. Incorporating an organic matrix into the biomimetic models resulted in absorption values ranging between ~25 % and ~40 % at 95 % RH (Fig. 6C), aligning with trends observed in natural eggshells. Further reductions in vapor absorption were achieved by integrating a lipid coating (Fig. 6D) [79]. However, the limited concentration of lipids in natural reptile cuticles limits its impact on the sorption properties [4,31,34,35]. Together, these findings support the hypothesis that while $CaCO_3$ is the dominant factor governing eggshell permeability, the organic matrix and lipid components modulate water vapor sorption within eggshells with low to moderate calcification.

The developed biomimetic models accurately reproduce the vapor sorption trends of representative reptile eggshells, demonstrating their ability to tune water vapor properties over a wide range. These models not only offer new insights into the interplay of eggshell components in regulating permeability but also provide a robust platform for designing materials with tailorable moisture absorption. Notably, this was achieved without the need for exact microstructural replication of the natural templates, highlighting that functional modularity and tunable sorption behavior can emerge from simplified, yet strategically designed, component integration.

3.4. Application potential

The developed biomimetic composites offer a bio-based, modular platform for the production of advanced materials with tunable sorption properties. This approach enables precise control over moisture uptake through modular design, rather than relying on synthetic polymers, fluorinated surface treatments, crosslinkers, or non-biodegradable additives, as is often the case in conventional moisture-regulating materials [13,23,53–56].

These characteristics open promising avenues for use in biomedical applications, particularly in wound healing and tissue engineering. The developed nanofibrous keratin membranes mimic the inner shell membrane of reptile eggs, which shares both structural and biochemical features with the human extracellular matrix [11–19]. The porous, interwoven fibrous network promotes gas exchange and provides a physical barrier against bacterial infiltration, while keratin's intrinsic properties—blood compatibility, biodegradability, and the presence of cell adhesion sequences—facilitate cell attachment and proliferation [11–13,19]. The tunable vapor sorption behavior of the composites is particularly valuable for addressing key limitations of conventional wound dressings. An effective dressing must balance fluid absorption with controlled moisture transmission to maintain an optimal healing environment—one that is moist enough to promote tissue regeneration but not so wet as to cause maceration [13,16,17]. In addition, adequate gaseous permeability—particularly for oxygen and carbon dioxide—is essential for cellular respiration during healing, underscoring the importance of porosity control in dressing design [13,16]. The incorporation of $CaCO_3$ into the biomimetic composites further allows tuning of the pore architecture and introduces calcium ions that can support bone regeneration, offering additional benefits for tissue engineering applications [18,22,54].

Beyond biomedical use, the biodegradability and tunable barrier properties of these composites also make them attractive for sustainable filtration and packaging applications [20,23,81]. Their biodegradable nature and customizable performance offer alternatives to petroleum-based or non-degradable materials, aligning with the growing demand for eco-friendly technologies [20–23,56,81].

Another key advantage of the biomimetic composites lies in exploring the broader multifunctionality observed in reptile eggshells. In addition to tunable gas and vapor sorption, natural eggshells exhibit antimicrobial, mechanical, and UV protection [3–5,9,10]. Future studies will explore whether similar tunability can be achieved for these material properties by adjusting the composition or morphology of our composites.

While the present work demonstrates tunable sorption performance, the system remains a simplified model with practical challenges. Such limitations include the loose deposition of the $CaCO_3$ layer and the need for stronger integration between modules. Additionally, while initial sorption results are promising, in vivo studies and durability testing in relevant environmental conditions are required to translate these materials from lab models to clinical or industrial use.

Despite these challenges, the present study highlights the potential of bioinspired, modular materials to deliver sustainable alternatives to current technologies. By expanding the structural complexity and functional tunability of these composites, we aim to approach the remarkable versatility of reptile eggshells and unlock new directions in material design.

4. Conclusion

This study demonstrates a modular biomimetic approach to designing keratin-based composites with tunable gaseous sorption properties. Inspired by the structural diversity of reptile eggshells, we systematically constructed key eggshell components—including electrospun keratin membranes, an organic matrix, a $CaCO_3$ layer, and a lipid coating—to develop bioinspired materials with controllable vapor absorption. The biomimetic models were benchmarked against representative reptile eggshells using Scanning Electron Microscopy (SEM) and Fourier-Transform Infrared (FTIR) spectroscopy, confirming the accuracy of their modular design.

Through Dynamic Vapor Sorption (DVS) analysis, we further validated this modular design strategy by demonstrating that the sorption behavior of the biomimetic composites closely aligns with representative eggshells from *Caiman crocodilus* (low absorption) and *Pantherophis guttatus* (high absorption). Additionally, we established that the $CaCO_3$ component is the dominant factor in modulating vapor absorption, as higher mineralization decreases sorption capacity. However, in composites with low $CaCO_3$ content, the organic matrix and lipid component play a crucial role in fine-tuning sorption properties, mimicking the nuanced sorption control observed in natural eggshells.

These findings highlight the potential of the bioinspired keratin-based composites as functional, tunable materials for applications that require precise moisture management. The combination of biocompatibility, biodegradability, and the ability to upcycle keratin-rich waste further enhances their relevance for sustainable wound dressings, tissue

engineering scaffolds, packaging, and filtration systems. This work underscores the value of a modular biomimetic design approach in engineering next-generation bioinspired materials with customizable properties.

CRediT authorship contribution statement

Yana Maudens: Writing – review & editing, Writing – original draft, Visualization, Validation, Methodology, Investigation, Formal analysis, Conceptualization. **Gerben Debruyn:** Writing – review & editing, Validation, Methodology, Formal analysis. **Eva Loccufier:** Writing – review & editing, Resources, Methodology. **Lode Daelemans:** Writing – review & editing, Supervision, Resources. **Erica Savino:** Writing – review & editing, Resources. **Cinzia Tonetti:** Writing – review & editing, Supervision, Resources. **Claudia Vineis:** Writing – review & editing, Supervision, Resources. **Alessio Varesano:** Writing – review & editing, Supervision, Resources. **Matthew D. Shawkey:** Writing – review & editing, Supervision, Resources, Methodology, Funding acquisition, Conceptualization. **Liliana D'Alba:** Writing – review & editing, Supervision, Resources, Methodology, Funding acquisition, Conceptualization. **Karen De Clerck:** Writing – review & editing, Supervision, Resources, Methodology, Funding acquisition, Conceptualization.

Funding

This work was supported by a Fonds voor Wetenschappelijk Onderzoek – Vlaanderen grant (GOA7921N) and European Office of Aerospace Research and Development grant (FA9655-23-1-7041). Additionally, Karen De Clerck and Liliana D'Alba would like to thank Ghent University, Belgium for its continued support of their research.

Declaration of competing interest

The authors declare that they have no known competing financial interests or personal relationships that could have appeared to influence the work reported in this paper.

Acknowledgements

We sincerely thank Phillipe Jouk, Curator Aquarium, Reptielen en Zeezoogdieren at the Antwerp Zoo, and Catherine Vancsok, Scientific Director of the Pairi Daiza Foundation, for facilitating access to the necessary eggshells, without which it would not have been possible to conduct this study. We thank Bernhard De Meyer for performing TGA analyses. We thank Laura Van Bossele for performing the XRD measurements and her assistance during analysis of the results. We are also grateful to Diego Omar Sánchez Ramírez for his help with the interpretation of the FTIR results. We gratefully acknowledge the team at the 'Werkplaats' of Ghent University, Faculty of Science, for their expertise in designing and manufacturing the solvent electrospin equipment. We are grateful for the financial support from the Universitaire Stichting van België.

Appendix A. Supplementary data

Supplementary data to this article can be found online at https://doi.org/10.1016/j.mtbio.2025.102032.

Data availability

The data underlying this article will be made available on request.

References

[1] P.P. Vijayan, D. Puglia, Biomimetic multifunctional materials: a review, Emergent Mater 2 (2019) 391–415, https://doi.org/10.1007/S42247-019-00051-7/FIGURES/15.
[2] J. Lin, X. Wang, B. Ding, J. Yu, G. Sun, M. Wang, Biomimicry via electrospinning, Crit. Rev. Solid State Mater. Sci. 37 (2012) 94–114, https://doi.org/10.1080/10408436.2011.627096.
[3] L. D'Alba, J. Goldenberg, A. Nallapaneni, D.Y. Parkinson, C. Zhu, B. Vanthournout, M.D. Shawkey, Evolution of eggshell structure in relation to nesting ecology in Non-avian reptiles, J. Morphol. 282 (2021) 1066–1079, https://doi.org/10.1002/JMOR.21347.
[4] L.J. Legendre, S. Choi, J.A. Clarke, The diverse terminology of reptile eggshell microstructure and its effect on phylogenetic comparative analyses, J. Anat. 241 (2022) 641–666, https://doi.org/10.1111/JOA.13723.
[5] M.J. Packard, V.G. DeMarco, Eggshell structure and formation in eggs of oviparous reptiles, Egg Incubation (1991) 53–70, https://doi.org/10.1017/CBO9780511585739.006.
[6] F. Liu, X. Jiang, Z. Chen, L. Wang, Mechanical design principles of Avian eggshells for survivability, Acta Biomater. 178 (2024) 233–243, https://doi.org/10.1016/J.ACTBIO.2024.02.036.
[7] N.R. Elejalde-Cadena, E. Hernández-Juárez, E. Tapia-Mendoza, A. Moreno, L. Bucio, Structural insights into ratite birds and crocodile eggshells for advanced biomaterials design, ACS Omega (2025), https://doi.org/10.1021/ACSOMEGA.4C10850.
[8] G. Debruyn, J. Geltmeyer, E. Schoolaert, M.P.J. Nicolaï, W. Xie, M. Wynant, M. D. Shawkey, K. De Clerck, L. D'Alba, Hydric environment and chemical composition shape Non-avian reptile eggshell absorption, Integr. Comp. Biol. 64 (2024) 107–119, https://doi.org/10.1093/ICB/ICAE040.
[9] H. Schleich, W. Kastle, M.J. Packard, Reptile egg-shells, SEM Atlas, 1988. New York.
[10] M. Packard, K. Hirsch, Scanning electron microscopy of eggshells of contemporary reptiles, Scanning Electron. Microsc. IV (1986) 1986. https://digitalcommons.usu.edu/electron/vol1986/iss4/34. (Accessed 2 December 2024).
[11] A. Vasconcelos, A. Cavaco-Paulo, Wound dressings for a proteolytic-rich environment, Appl. Microbiol. Biotechnol. 90 (2011) 445–460, https://doi.org/10.1007/S00253-011-3135-4/TABLES/6.
[12] M. Zhai, Y. Xu, B. Zhou, W. Jing, Keratin-chitosan/n-ZnO nanocomposite hydrogel for antimicrobial treatment of burn wound healing: characterization and biomedical application, J. Photochem. Photobiol., B 180 (2018) 253–258, https://doi.org/10.1016/J.JPHOTOBIOL.2018.02.018.
[13] A. Noor, A. Afzal, R. Masood, Z. Khaliq, S. Ahmad, F. Ahmad, M.B. Qadir, M. Irfan, Dressings for burn wound: a review, J. Mater. Sci. 57 (12) (2022) 6536–6572, https://doi.org/10.1007/S10853-022-07056-4, 57 (2022).
[14] Y. Liu, Q. Guo, X. Zhang, Y. Wang, X. Mo, T. Wu, Progress in electrospun fibers for manipulating cell behaviors, Advanced Fiber Materials 5 (2023) 1241–1272, https://doi.org/10.1007/S42765-023-00281-9/FIGURES/15.
[15] G.G. Flores-Rojas, B. Gómez-Lazaro, F. López-Saucedo, R. Vera-Graziano, E. Bucio, E. Mendizábal, Electrospun scaffolds for tissue engineering: a review, Macromol 3 (2023) 524–553, https://doi.org/10.3390/MACROMOL3030031.
[16] F. Feng, Z. Zhao, J. Li, Y. Huang, W. Chen, Multifunctional dressings for wound exudate management, Prog. Mater. Sci. 146 (2024), https://doi.org/10.1016/J.PMATSCI.2024.101328.
[17] M.F.P. Graça, D. de Melo-Diogo, I.J. Correia, A.F. Moreira, Electrospun asymmetric membranes as promising wound dressings: a review, Pharmaceutics 13 (2021) 1–25, https://doi.org/10.3390/PHARMACEUTICS13020183.
[18] Y. zhuo Huang, Y. rong Ji, Z. wen Kang, F. Li, S. fang Ge, D.P. Yang, J. Ruan, X. qun Fan, Integrating eggshell-derived CaCO3/MgO nanocomposites and chitosan into a biomimetic scaffold for bone regeneration, Chem. Eng. J. 395 (2020) 125098, https://doi.org/10.1016/J.CEJ.2020.125098.
[19] X. Chen, Y. Chen, B. Fu, K. Li, D. Huang, C. Zheng, M. Liu, D.P. Yang, Eggshell membrane-mimicking multifunctional nanofiber for in-situ skin wound healing, Int. J. Biol. Macromol. 210 (2022) 139–151, https://doi.org/10.1016/J.IJBIOMAC.2022.04.212.
[20] F. Aghababaei, D.J. McClements, M.M. Martinez, M. Hadidi, Electrospun plant protein-based nanofibers in food packaging, Food Chem. 432 (2024), https://doi.org/10.1016/J.FOODCHEM.2023.137236.
[21] L. Zhao, G. Duan, G. Zhang, H. Yang, S. Jiang, S. He, Electrospun functional materials toward food packaging applications: a review, Nanomaterials 10 (2020), https://doi.org/10.3390/NANO10010150.
[22] X. Zhang, M. Liu, Z. Kang, B. Wang, B. Wang, F. Jiang, X. Wang, D.P. Yang, R. Luque, NIR-triggered photocatalytic/photothermal/photodynamic water remediation using eggshell-derived CaCO3/CuS nanocomposites, Chem. Eng. J. 388 (2020) 124304, https://doi.org/10.1016/J.CEJ.2020.124304.
[23] S.A. Siddiqui, A. Sundarsingh, N.A. Bahmid, N. Nirmal, J.F.M. Denayer, K. Karimi, A critical review on biodegradable food packaging for meat: materials, sustainability, regulations, and perspectives in the EU, Compr. Rev. Food Sci. Food Saf. 22 (2023) 4147–4185, https://doi.org/10.1111/1541-4337.13202.
[24] Y. Chang, P.Y. Chen, Hierarchical structure and mechanical properties of snake (Naja atra) and turtle (Ocadia sinensis) eggshells, Acta Biomater. 31 (2016) 33–49, https://doi.org/10.1016/J.ACTBIO.2015.11.040.
[25] H.J. Wu, Y.C. Tseng, S.H. Tsao, P.L. Chiang, W.Y. Tai, H.I. Hsieh, H.T. Yu, J. Y. Juang, A comparative study on the microstructures, mineral content, and mechanical properties of non-avian reptilian eggshells, Biology 12 (2023) 688, https://doi.org/10.3390/BIOLOGY12050688, 12 (2023) 688.

[26] M.L.H. Rose, M.T. Hincke, Protein constituents of the eggshell: eggshell-specific matrix proteins, Cell. Mol. Life Sci. 66 (2009) 2707–2719, https://doi.org/10.1007/S00018-009-0046-Y/FIGURES/4.
[27] B.D. Palmer, V.G. Demarco, L.J. Guillette, Oviductal morphology and eggshell formation in the lizard, Sceloporus woodi, J. Morphol. 217 (1993) 205–217, https://doi.org/10.1002/JMOR.1052170208.
[28] M.T. Hincke, Y. Nys, J. Gautron, K. Mann, A.B. Rodriguez-Navarro, M.D. McKee, The eggshell: structure, composition and mineralization, Front. Biosci. 17 (2012) 1266–1280, https://doi.org/10.2741/3985/PDF.
[29] H. Silyn-Roberts, R.M. Sharp, Preferred orientation of calcite and aragonite in the reptilian eggshells, Proc. R. Soc. Lond. B Biol. Sci. 225 (1985) 445–455, https://doi.org/10.1098/RSPB.1985.0072.
[30] S. Choi, S. Han, N.H. Kim, Y.N. Lee, A comparative study of eggshells of Gekkota with morphological, chemical compositional and crystallographic approaches and its evolutionary implications, PLoS One 13 (2018) e0199496, https://doi.org/10.1371/JOURNAL.PONE.0199496.
[31] G. Kulshreshtha, L. D'Alba, I.C. Dunn, S. Rehault-Godbert, A.B. Rodriguez-Navarro, M.T. Hincke, Properties, genetics and innate immune function of the cuticle in egg-laying species, Front. Immunol. 13 (2022) 838525, https://doi.org/10.3389/FIMMU.2022.838525/BIBTEX.
[32] A.B. Rodríguez-Navarro, N. Domínguez-Gasca, A. Muñoz, M. Ortega-Huertas, Change in the chicken eggshell cuticle with hen age and egg freshness, Poult. Sci. 92 (2013) 3026–3035, https://doi.org/10.3382/PS.2013-03230.
[33] D.C. Fecheyr-Lippens, B. Igic, L. D'Alba, D. Hanley, A. Verdes, M. Holford, G.I. N. Waterhouse, T. Grim, M.E. Hauber, M.D. Shawkey, The cuticle modulates ultraviolet reflectance of avian eggshells, Biol Open 4 (2015) 753–759, https://doi.org/10.1242/BIO.012211.
[34] L. D'Alba, R. Torres, G.I.N. Waterhouse, C. Eliason, M.E. Hauber, M.D. Shawkey, What does the eggshell cuticle do? A functional comparison of Avian eggshell cuticles, Physiol. Biochem. Zool. 90 (2017) 588–599, https://doi.org/10.1086/693434.
[35] R.C. Noble, Egg Incubation: Its Effects on Embryonic Development in Birds and Reptiles, Cambridge University Press, 1991.
[36] C.R. Tracy, Water relations of parchment-shelled lizard (Sceloporus undulatus) eggs, Copeia 1980 (1980) 478, https://doi.org/10.2307/1444525.
[37] D.C. Deeming, M.B. Thompson, Egg incubation: gas exchange across reptilian eggshells, Egg Incubation (1991) 277–284, https://doi.org/10.1017/CBO9780511585739.018.
[38] R.M. Andrews, Rigid shells enhance survival of gekkotan eggs, J Exp Zool A Ecol Genet Physiol 323 (2015) 607–615, https://doi.org/10.1002/JEZ.1951.
[39] R.A. Ackerman, R.C. Seagrave, R. Dmi'el, A. Ar, Water and heat exchange between parchment-shelled reptile eggs and their surroundings, Copeia 1985 (1985) 703–711, https://doi.org/10.2307/1444764.
[40] M.J. Packard, G.C. Packard, T.J. Boardman, Structure of eggshells and water relations of reptilian eggs, Herpetologica 38 (1982) 136–155.
[41] D.C. Deeming, Nesting environment may drive variation in eggshell structure and egg characteristics in the Testudinata, J Exp Zool A Ecol Integr Physiol 329 (2018) 331–342, https://doi.org/10.1002/JEZ.2169.
[42] M.B. Thompson, Water exchange in reptilian eggs, Physiol. Zool. 60 (1987) 1–8. http://www.jstor.org/stable/30158623.
[43] G.C. Grigg, Water relations of crocodilian eggs: management considerations, in: Wildlife Management: Crocodiles and Alligators, Surrey Beatty and Sons Pty Limited in association with the Conservation Commission of the Northern Territory, 1987, pp. 499–502.
[44] D.C. Deeming, M. Ruta, Egg shape changes at the theropod-bird transition, and a morphometric study of amniote eggs, R. Soc. Open Sci. 1 (2014), https://doi.org/10.1098/RSOS.140311.
[45] D.O.S. Ramirez, I. Cruz-Maya, C. Vineis, V. Guarino, C. Tonetti, A. Varesano, Wool keratin-based nanofibres—in vitro validation, Bioengineering 8 (2021) 224, https://doi.org/10.3390/BIOENGINEERING8120224, 8 (2021) 224.
[46] D.O. Sanchez Ramirez, C. Vineis, I. Cruz-Maya, C. Tonetti, V. Guarino, A. Varesano, Wool keratin nanofibers for bioinspired and sustainable use in biomedical field, J. Funct. Biomater. 14 (2022), https://doi.org/10.3390/JFB14010005.
[47] D.O. Sanchez Ramirez, I. Cruz-Maya, C. Vineis, C. Tonetti, A. Varesano, V. Guarino, Design of asymmetric nanofibers-membranes based on polyvinyl alcohol and wool-keratin for wound healing applications, J. Funct. Biomater. 12 (2021), https://doi.org/10.3390/JFB12040076.
[48] A. Akhmetova, A. Heinz, Electrospinning proteins for wound healing purposes: opportunities and challenges, Pharmaceutics 13 (2020) 4, https://doi.org/10.3390/PHARMACEUTICS13010004.
[49] B. Abadi, N. Goshtasbi, S. Bolourian, J. Tahsili, M. Adeli-Sardou, H. Forootanfar, Electrospun hybrid nanofibers: fabrication, characterization, and biomedical applications, Front. Bioeng. Biotechnol. 10 (2022) 986975, https://doi.org/10.3389/FBIOE.2022.986975.
[50] S. Mowafi, H. El-Sayed, Production and utilization of keratin and sericin-based electro-spun nanofibers: a comprehensive review, J. Nat. Fibers 20 (2023), https://doi.org/10.1080/15440478.2023.2192544.
[51] J. Xue, J. Xie, W. Liu, Y. Xia, Electrospun nanofibers: new concepts, materials, and applications, Acc. Chem. Res. 50 (2017) 1976–1987, https://doi.org/10.1021/ACS.ACCOUNTS.7B00218.
[52] J. Xue, T. Wu, Y. Dai, Y. Xia, Electrospinning and electrospun nanofibers: methods, materials, and applications, Chem. Rev. 119 (2019) 5298–5415, https://doi.org/10.1021/ACS.CHEMREV.8B00593.
[53] E. Loccufier, J. Geltmeyer, L. Daelemans, D.R. D, K. De Buysser, K. De Clerck, E. Loccufier, J. Geltmeyer, L. Daelemans, K. De Clerck, K. De Buysser, Silica nanofibrous membranes for the separation of heterogeneous azeotropes, Adv. Funct. Mater. 28 (2018) 1804138, https://doi.org/10.1002/ADFM.201804138.
[54] H. Reuvekamp, E.E.G. Hekman, E. van der Heide, D.T.A. Matthews, Strategies in surface engineering for the regulation of microclimates in skin-medical product interactions, Heliyon 10 (2024) e25395, https://doi.org/10.1016/J.HELIYON.2024.E25395.
[55] X. Li, W. Guo, P.C. Hsu, Personal thermoregulation by moisture-engineered materials, Adv. Mater. 36 (2024) 2209825, https://doi.org/10.1002/ADMA.202209825. CSUBTYPE:STRING:SPECIAL;PAGE:STRING:ARTICLE/CHAPTER.
[56] J. Kim, S. Kim, S.Y. Woo, H. Chun, J. Sim, S. Kang, K. Min, In-situ analysis of water transport properties through a reinforced composite membrane in polymer electrolyte membrane fuel cells, Chem. Eng. J. 502 (2024) 158078, https://doi.org/10.1016/J.CEJ.2024.158078.
[57] R.R. Yan, J.S. Gong, C. Su, Y.L. Liu, J.Y. Qian, Z.H. Xu, J.S. Shi, Preparation and applications of keratin biomaterials from natural keratin wastes, Appl. Microbiol. Biotechnol. 106 (2022) 2349–2366, https://doi.org/10.1007/S00253-022-11882-6.
[58] A. Varesano, C. Vineis, C. Tonetti, D. Ramirez, G. Mazzuchetti, S. Ortelli, M. Blosi, A. Costa, Multifunctional hybrid nanocomposite nanofibers produced by colloid electrospinning from water solutions, Curr. Nanosci. 11 (2014) 41–48, https://doi.org/10.2174/15734137106661409222250 56.
[59] A. Varesano, C. Vineis, C. Tonetti, D.O.S. Ramírez, G. Mazzuchetti, Chemical and physical modifications of electrospun keratin nanofibers induced by heating treatments, J. Appl. Polym. Sci. 131 (2014), https://doi.org/10.1002/APP.40532.
[60] S.J. Eichhorn, W.W. Sampson, Relationships between specific surface area and pore size in electrospun polymer fibre networks, J. R. Soc. Interface 7 (2009) 641, https://doi.org/10.1098/RSIF.2009.0374.
[61] K. Damaziak, A. Marzec, Analysis of ultrastructure and microstructure of blackbird (Turdus merula) and song thrush (Turdus philomelos) eggshell by scanning electron microscopy and X-ray computed microtomography, Sci. Rep. 12 (2022), https://doi.org/10.1038/S41598-022-16033-5.
[62] W.H. Han, M.Q. Wang, J.X. Yuan, C.C. Hao, C.J. Li, Y.Z. Long, S. Ramakrishna, Electrospun aligned nanofibers: a review, Arab. J. Chem. 15 (2022) 104193, https://doi.org/10.1016/J.ARABJC.2022.104193.
[63] G. Debruyn, S. Choi, J.L. Dobson, Y. Maudens, K. De Clerck, M.D. Shawkey, S. Zhang, L. D'Alba, Convergence in biomineralization patterns across animal eggshells, Faraday Discuss (2024), https://doi.org/10.1039/D5FD00028A.
[64] J. Deering, V. Nelea, M.D. McKee, Multiscale mineralization in the leopard gecko eggshell, Adv. Funct. Mater. 34 (2024), https://doi.org/10.1002/ADFM.202316422.
[65] J. Chen, M. Jiang, M. Su, J. Han, S. Li, Q. Wu, Mineralization of calcium carbonate induced by egg substrate and an electric field, Chem. Eng. Technol. 42 (2019) 1525–1532, https://doi.org/10.1002/CEAT.201800509.
[66] M. Di Foggia, A. Torreggiani, P. Taddei, M. Dettin, A. Tinti, Self-assembling peptides for biomedical applications: IR and Raman spectroscopies for the study of secondary structure, Proteonomics Res. J. 2 (2012). https://www.researchgate.net/publication/286101944_Self-assembling_peptides_for_biomedical_applications_IR_and_Raman_spectroscopies_for_the_study_of_secondary_structure. (Accessed 25 November 2024).
[67] A. Fallahi, M. Barmar, M.H. Kish, Preparation of phase-change material microcapsules with paraffin or camel fat cores: application to fabrics, Iran. Polym. J. (Engl. Ed.) (2010). https://www.magiran.com/p723572. (Accessed 25 November 2024).
[68] D. Varshney, M. Ahmadi, M.J.F. Guinel, B.R. Weiner, G. Morell, Single-step route to diamond-nanotube composite, Nanoscale Res. Lett. 7 (2012), https://doi.org/10.1186/1556-276X-7-535.
[69] M. Tizo, L. Blanco, A. Cagas, B. Cruz, J. Encoy, J. Gunting, R. Arazo, V.I. Mabayo, Efficiency of calcium carbonate from eggshells as an adsorbent for Cadmium removal in aqueous solution, Sustain. Environ. Res. (2018), https://doi.org/10.1016/j.serj.2018.09.002.
[70] N.R. Elejalde-Cadena, D. Hernández, F. Capitelli, S.R. Islas, M.J. Rosales-Hoz, M. Zema, S.C. Tarantino, D. Siliqi, A. Moreno, Influence of intramineral proteins on the growth of carbonate crystals using as a scaffold membranes of ratite birds and crocodiles eggshells, Membranes 13 (2023), https://doi.org/10.3390/MEMBRANES13110869.
[71] D. Gebauer, P.N. Gunawidjaja, J.Y.P. Ko, Z. Bacsik, B. Aziz, L. Liu, Y. Hu, L. Bergström, C.W. Tai, T.K. Sham, M. Edén, N. Hedin, Proto-calcite and proto-vaterite in amorphous calcium carbonates, Angew. Chem., Int. Ed. 49 (2010) 8889–8891, https://doi.org/10.1002/ANIE.201003220.
[72] M. Farhadi-Khouzani, D.M. Chevrier, P. Zhang, N. Hedin, D. Gebauer, Water as the key to proto-aragonite amorphous CaCO3, Angew. Chem. Int. Ed. 55 (2016) 8117–8120, https://doi.org/10.1002/ANIE.201603176.
[73] M. Ni, B.D. Ratner, Differentiation of calcium carbonate polymorphs by surface analysis techniques – an XPS and TOF-SIMS study, Surf. Interface Anal. 40 (2008) 1356, https://doi.org/10.1002/SIA.2904.
[74] S.L. Shamblin, B.C. Hancock, G. Zografi, Water vapor sorption by peptides, proteins and their formulations, Eur. J. Pharm. Biopharm. 45 (1998) 239–247, https://doi.org/10.1016/S0939-6411(98)00006-X.
[75] E. Senoz, R.P. Wool, C.W.J. McChalicher, C.K. Hong, Physical and chemical changes in feather keratin during pyrolysis, Polym. Degrad. Stabil. 97 (2012) 297–307, https://doi.org/10.1016/J.POLYMDEGRADSTAB.2011.12.018.
[76] C. Sangwichien, G.L. Aranovich, M.D. Donohue, Density functional theory predictions of adsorption isotherms with hysteresis loops, Colloids Surf. A Physicochem. Eng. Asp. 206 (2002) 313–320, https://doi.org/10.1016/S0927-7757(02)00048-1.

[77] I.C. Watt, Sorption of water vapor by keratin, Journal of Macromolecular Science—Reviews in Macromolecular Chemistry 18 (1980) 169–245, https://doi.org/10.1080/00222358008081042.
[78] Y. Hu, Q. Yu, Experimental and theoretical studies on water adsorption and capillary condensation in nanopores of calcium carbonate, Geoenergy Sci. Eng. 236 (2024), https://doi.org/10.1016/J.GEOEN.2024.212740.
[79] Q. Tan, M. Zhou, Z. Chen, F. Hu, H. Zhang, Y. Chen, Oxidation modification of paraffin wax and preparation of water-repellent finish emulsion, Fibers Polym. 25 (2024) 2389–2402, https://doi.org/10.1007/S12221-024-00567-8/FIGURES/12.
[80] S. Samiullah, J.R. Roberts, The eggshell cuticle of the laying hen, Worlds Poult. Sci. J. 70 (2014) 693–708, https://doi.org/10.1017/S0043933914000786.
[81] Y. Kang, Z.X. Low, D. Zou, Z. Zhong, W. Xing, Multifunctional nanofibrous membranes for integrated air purification, Advanced Fiber Materials 6 (5) (2024) 1306–1342, https://doi.org/10.1007/S42765-024-00427-3, 6 (2024.